Data in Brief 63 (2025) 112308

Contents lists available at ScienceDirect

Data in Brief

journal homepage: www.elsevier.com/locate/dib

Data Article

Experimental dataset of charge and discharge patterns in a 1200Ah OpzS battery bank ☆

Javier Rocha [a,*], Ricardo Aguasca [b], Máximo Méndez [c]

[a] PhD candidate in the PhD Program in Telecommunications Technologies and Computational Engineering (SIANI) at the University of Las Palmas de Gran Canaria (ULPGC), Spain
[b] Department of Electronic and Automatic Engineering, SIANI - Evolutionary Computation and Applications (CEANI), University of Las Palmas de Gran Canaria (ULPGC), Spain
[c] Department of Computer Science and Systems, SIANI - Evolutionary Computation and Applications (CEANI), University of Las Palmas de Gran Canaria (ULPGC), Spain

A R T I C L E I N F O

Article history:
Received 4 October 2025
Revised 11 November 2025
Accepted 17 November 2025
Available online 20 November 2025

Dataset link: Experimental Dataset Patterns in a 1200Ah Battery (Original data)

Keywords:
Probabilistic genetic algorithms
OPzS lead-acid batteries
State of charge estimation
Voltage prediction
Renewable energy storage

A B S T R A C T

This dataset was generated from experiments on a bank of six 1200 Ah OPzS stationary batteries connected in series to form a 12 V storage system. Each cell was monitored for voltage, temperature, and electrolyte density using a DataTaker DT85M recorder, complemented by Pt100, analog voltmeters, and Hall effect sensors. Charging was performed with a programmable DC power supply under conventional, photovoltaic, and wind profiles, while discharging used a programmable electronic load capable of reproducing C10 and C20 curves, real consumption patterns from Gran Canaria, and random pulse sequences.
Data were collected at one-minute intervals between August 2024 and May 2025, covering 1375 h and 42 min. The dataset includes 14 charge–discharge cycles, with 1053 to 13,385 records per cell. Provided in CSV format, the dataset enables straightforward processing and supports applications in battery modeling, comparative performance analysis, and validation of energy management algorithms.

☆ Instituto Universitario de Sistemas Inteligentes y Aplicaciones Numéricas en la Ingeniería (SIANI). Edificio Polivalente I. Universidad de Las Palmas de Gran Canaria, Science and Technology Park. Practicante Ignacio Rodríguez Street, S/N, 35017, Las Palmas de Gran Canaria, Spain.

* Corresponding author.
E-mail addresses: francisco.rocha101@alu.ulpgc.es (J. Rocha), ricardo.aguasca@ulpgc.es (R. Aguasca), maximo.mendez@ulpgc.es (M. Méndez).

https://doi.org/10.1016/j.dib.2025.112308

Specifications Table

Subject	Engineering & Materials science
Specific subject area	Evolution of the voltage, current, temperature, capacity and state of charge parameters of a high-power stationary lead-acid battery.
Type of data	Table (.csv format) Variables obtained by an industrial data logger that transfers the values of the voltage, temperature and current sensors that it creates in a temporary database every minute.
Data collection	Each cell of the 1200 Ah OPzS stationary accumulator was equipped with individual sensors for measuring electrical and physical-chemical parameters, specifically voltage, temperature, and current. These devices were integrated into a data acquisition system based on the DataTaker DT85M industrial recorder, complemented by Pt100 temperature sensors, analog voltmeters, and Hall effect sensors for current monitoring. The charging process was carried out using a Magna Power SL100–15/UI programmable direct current source, which allowed emulation of both the charging patterns specified by the manufacturer and photovoltaic and wind generation profiles. The discharge process was controlled by a 6 kW Adaptive Power 5VP06–42C programmable electronic load, capable of reproducing C10 and C20 regimes, in addition to consumption profiles characteristic of the island of Gran Canaria and random pulse sequences. The management and visualization of the experimental data was carried out using the recorder's dEX 2.0 software, and they were subsequently adapted for processing in CSV format,
Data source location	Circuits and Power Electronics Laboratory of the School of Telecommunications and Electronics Engineering (EITE), ULPGC, Tafira Baja, Las Palmas, Canary Islands, Spain. GPS coordinates: 28.071111111111, −15.453611111111.
Data accessibility	Repository name: Zenodo. Data identification number: ⟨13:italic ⟩https://doi.org/10.5281/zenodo.17252822⟨/13:italic⟩ Direct URL to data: https://zenodo.org/records/17252822 Instructions for accessing these data: Structure of the dataset, called 'Experimental dataset of charge and discharge patterns in a 1200 Ah OpzS battery bank'. Within the same folder there are six ZIP compressed subfolders (cells 1 to 6). After decompressing the ZIP files, each subfolder contains data from an OPzS battery cell, with 15 data files for cell 1 and 19 data files for cells 2 to 6, representing the different charge and discharge pattern tests performed. Each file is named according to the following structure: "Cell measurements N – Ordinal number of the test – Type of charge pattern – Type of discharge pattern," where N represents the cell number. The 19 files for each cell, with the exception of cell 1, which has unified the photovoltaic measurements on clear and cloudy days, resulting in 15 files.
Related research article	*T*he XXXVIII ENDIO – XXXVI EPIO conference proceedings are currently pending publication (#16): https://epio.org.ar/endio-epio-2025/trabajos-Sincronica-remota-1/

1. Value of the Data

The main beneficiaries of this experimental work are researchers working on high-capacity stationary lead–acid battery systems and their applications. The dataset may also benefit engineers and professionals involved in integrating such storage systems into renewable energy applications—particularly photovoltaic and wind systems—as well as those developing and optimizing electrical microgrids [1,3,8]. Systematic recording of experimental parameters is essential for modeling high-capacity lead–acid batteries, since most existing datasets focus on smaller systems. In this work, measurements were obtained using calibrated and highly reliable equipment, ensuring data accuracy and enabling validation of battery models by comparing experimental and simulated results. The controlled tests performed on a 1200 Ah OPzS stationary battery provide a transferable scientific resource that goes beyond case-specific analyses.

The dataset can be reused for:

(i) electrical and electrochemical modeling for equivalent circuit calibration;
(ii) validation of state-of-charge (SOC) and state-of-health (SOH) algorithms;
(iii) studies of degradation and lifetime;
(iv) evaluation of energy management strategies;
(v) artificial intelligence applications for anomaly detection and prediction;
(vi) interlaboratory benchmarking for protocol comparison and standardization.

2. Background

The primary motivation for generating this dataset was the development of advanced modeling methodologies for energy storage systems based on lead–acid batteries [5–7]. The objective is to optimize these models through the use of genetic algorithms [2], with the goal of improving their dynamic representation and predictive accuracy under real-world operating conditions. This work is particularly relevant in the context of microgrids with renewable energy integration [4], where efficient storage management is essential to maintain system stability and maximize energy utilization. The experimental data presented here not only provide a robust foundation for validating optimization models and algorithms but also constitute a key element of a broader research effort aimed at improving the design, control, and operation of stationary storage batteries in distributed energy applications. Importantly, very few experimental datasets are available for high-capacity OPzS batteries, which makes this contribution a unique and valuable resource for the research community [9,10,12].

3. Data Description

There are six folders (Cell 1 to Cell 6), each corresponding to one of the battery cells. Within each folder, fifteen (Cell 1) and nineteen (Cell 2 to 6) data files are provided, representing the different charge and discharge tests performed.

The experiments were performed using batteries in factory-new condition. Therefore, the initial state of health (SoH_n) was equal to 1 [11]. After electrolyte filling, the tests were initiated.

In each cell's first CSV file, measurements from the initial charge–discharge cycle are recorded. Column 6 contains the initial capacity value (Q_n) expressed in ampere-hours (Ah), while Column 7 shows the initial state of charge ($\%SoC_n$), which evolves throughout the experiment.

Accordingly, the values in the last row of each CSV file represent the results at the end of that specific test cycle. These results serve as the initial conditions for the following charge–discharge cycle, and the same approach is maintained for all subsequent cycles.

Each file is named according to the following structure: Cell measurements N – Test ordinal number – Charge pattern type – Discharge pattern type, where N denotes the cell number. All files are provided in comma-separated values format (CSV extension). The delimiter used is a semicolon (;), which ensures clear separation of fields across columns. This format is widely compatible with data analysis software, databases, and programming languages such as MATLAB and Python, and facilitates data exchange between different applications.

Each file consists of a single main table, containing N records distributed across seven columns, organized in a clear tabular structure. In total, the dataset comprises **579,448 individual records** (about 96,500 per cell), distributed across the 19 experimental cycles. The number of records per cycle varies substantially, ranging from around **1053 to 13,385 entries per cell** (equivalent to 6318 to 80,310 records when considering all six cells), reflecting the different durations and operating conditions of the tests.

The dataset is therefore arranged in a straightforward and consistent manner, which supports efficient access, processing, and reuse in diverse analytical environments.

The columns are:

Column	Structural description	Format
Timestamp	Timestamp with one-minute resolution.	[DD/MM/YYYY hh:mm]
Vn (mV)	Voltage values in millivolts.	[XXXX,XX]
Vn (V)	Voltage values in volts (adjusted magnitude).	[X,XXXXX]
Tn (°C)	Temperature values in degrees Celsius.	[XX,XX]
I (A)	Current in amperes (+ charge / - discharge).	[±XXX,XX]
(Ah)	Accumulated magnitude in ampere-hours.	[XXXX,XX]
%SOC	State of Charge percentage.	[XXX,XX]

NOTE: The value ‘n’ indicates the cell number.

Conceptual example of a CSV:

A table like this in Excel:

Timestamp	V1 (mV)	V1 (V)	T1 (°C)	I (A)	(Ah)	%SOC
28/08/2024 9:30	2094,36	2,09,436	25,06	10,10	0,17	0,00 %
05/09/2024 18:02	2304,65	2,30,465	26	1,94	633,56	53 %
24/09/2024 18:00	2293,85	2,29,385	25,48	−10,01	633,39	53 %

Saved in CSV format, the text file would look like this:
Timestamp; V1 (mV); V1 (V); T1 (°C ; I (A); (Ah); %SOC
28/08/2024 9:30; 2094,36; 2,09,436; 25,06; 10,10; 0,17; 0,00 %
05/09/2024 18:02; 2304,65; 2,30,465; 26; 1,94; 633,56; 53 %
24/09/2024 18:00; 2293,85; 2,29,385; 25,48; −10,01; 633,39; 53 %

4. Experimental Design, Materials and Methods

The experimental setup was configured as illustrated in Fig. 1. The acquisition system included voltage and temperature sensors connected to a DataTaker DT85M data logger (Fig. 2).

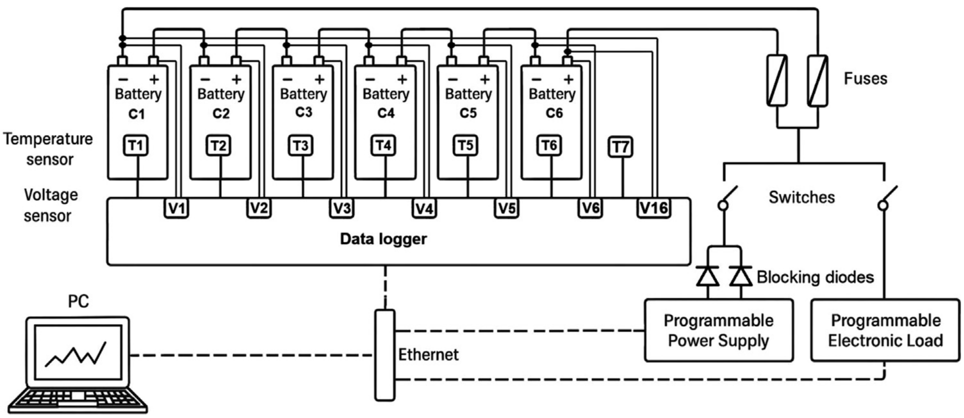

Fig. 1. General configuration of the experimental setup for charge and discharge tests.

Fig. 2. DataTaker DT85M data logger connected to the acquisition system.

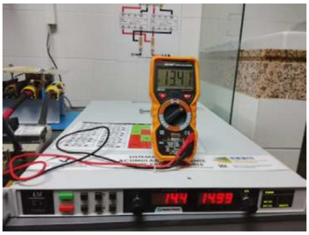

Fig. 3. Magna Power SL100–15/UI programmable DC power supply used for charging.

Fig. 4. Protection system with parallel power-blocking diodes.

Fig. 5. Switching and current-limiting system with NH fuses and four-pole disconnectors.

The logger, linked to the local area network (LAN), integrated and processed the collected signals. Data management was carried out through the dEX 2.0 application, which handled logger requests, extracted sensor readings, and stored the information in a database via a 10-meter LAN connection.

For charging, a Magna Power SL100–15/UI programmable DC power supply was used (Fig. 3). This equipment allowed the reproduction of conventional charging profiles as well as photovoltaic and wind patterns. System protection was implemented through parallel power-blocking diodes (Fig. 4).

Table 1
Parameters of the operating protocol for charge and discharge cycles.

Combination	Switch K1	Switch K2	Parámetro
1	OFF	OFF	K1 and K2 are deactivated, the battery is empty.
2	OFF	ON	Only K2 activated, battery is charging.
3	ON	OFF	Only K1 activated, the battery is discharged.
4	ON	ON	K1 and K2 activated, prohibited combination.

Fig. 6. Adaptive Power 5VP06–42C programmable electronic load used for discharging.

Fig. 7. Experimental bench consisting of six 1200 Ah, 2 V OPzS lead–acid stationary batteries.

A switching and current-limiting system was also integrated into the power line, consisting of European NH blade fuses and four-pole disconnectors, K1 and K2 (Fig. 5). By operating the rotary knob, the circuit could be closed (1, "ON") or opened (0, "OFF"), enabling or interrupting current flow according to the specified operating protocol. This protocol covered both charging and scheduled discharging of the batteries, as defined in Table 1.

The discharging process was carried out using a 6 kW Adaptive Power 5VP06–42C programmable electronic load (Fig. 6). This equipment allowed the reproduction of C10 and C20 discharge curves, real consumption profiles from Gran Canaria, and pulse sequences consisting of 10 min at a constant high current followed by 20 min without current. Data management and visualization were performed with dEX 2.0, the proprietary software of the recorder, in combination with Microsoft Excel.

Finally, the experimental bench consisted of six stationary OPzS lead–acid batteries, each rated at 1200 Ah and 2 V (Fig. 7). Together, the integrated charging, discharging, monitoring, and protection systems provided a controlled yet realistic experimental environment, ensuring reliable and high-quality data for analysis and reuse.

4.1. Data acquisition methodology

The study was conducted under different operating regimes and thermal conditions in order to characterize the system's dynamic response. A total of 15 (Cell 1) and 19 (Cells 2 to 6) charge

Table 2a
Experimental summary for cell 1.

File	Number of records	Duration (Hour/min.)
Cell 1 Measurements - First Charge-C20 discharge.csv	13,385	223/05
Cell 1 Measurements - Second Charge-C20 discharge.csv	9905	165/05
Cell 1 Measurements - Third Charge-C20 discharge.csv	8502	141/42
Cell 1 Measurements - Fourth Load-C20 discharge.csv	9878	164/38
Cell 1 Measurements - Fifth Load-C10 discharge.csv	9389	156/29
Cell 1 Measurements - Sixth Load-C10 discharge.csv	10,153	169/13
Cell 1 Measurements - Seventh and Eighth Photovoltaic Load clear - C20 discharge.csv	4746	79/06
Cell 1 Measurements - Seventh and Eighth Photovoltaic Load Cloudy - C20 discharge.csv	4782	79/42
Cell 1 Measurements - Ninth and Tenth Photovoltaic Load Clear - C10 discharge.csv	3259	54/19
Cell 1 Measurements - Ninth and Tenth Photovoltaic Load Cloudy - C10 discharge.csv	2710	45/10
Cell 1 Measurements - Eleventh Load - GC discharge.csv	8196	136/36
Cell 1 Measurements - Twelfth Photovoltaic Load cleared - GC discharge.csv	5757	95/57
Cell 1 Measurements - Twelfth Photovoltaic Load Cloudy - GC discharge.csv	5757	95/57
Cell 1 Measurements - Thirteenth Load wind energy - GC discharge.csv	2819	46/59
Cell 1 Measurements - Fourteenth Load - Discharge Pulses.csv	5931	98/51

and discharge cycles were carried out, with data recorded at a frequency of one data point per minute.

The experimental phases are detailed in Tables 2a (Cell 1) and 2b (Cells 2 to 6), which summarizes the dataset obtained through continuous monitoring. Data collection was performed at one-minute intervals between August 28, 2024, at 09:30 a.m. and May 5, 2025, at 05:34 pm., resulting in a total duration of 9657 h and 28 min, comprising **579,448 recorded data points**. Table 2b

Table 2b
Experimental summary for cells 2 to 6.

Cell	File	Number of records	Duration (Hour/min.)
2	Cell 2 Measurements - First Charge-C20 discharge.csv	13,385	223/05
	Cell 2 Measurements - Second Charge-C20 discharge.csv	9905	165/05
	Cell 2 Measurements - Third Charge-C20 discharge.csv	8493	141/33
	Cell 2 Measurements - Fourth Load-C20 discharge.csv	9878	164/38
	Cell 2 Measurements - Fifth Load-C10 discharge.csv	9388	156/28
	Cell 2 Measurements - Sixth Load-C10 discharge.csv	10,153	169/13
	Cell 2 Measurements - Seventh Photovoltaic Load clear - C20 discharge.csv	1848	30/48
	Cell 2 Measurements - Eighth Photovoltaic Load clear - C20 discharge.csv	1849	30/49
	Cell 2 Measurements - Seventh Photovoltaic Load Cloudy - C20 discharge.csv	1849	30/49
	Cell 2 Measurements - Eighth Photovoltaic Load Cloudy - C20 discharge.csv	1895	31/35
	Cell 2 Measurements - Ninth Photovoltaic Load clear - C10 discharge.csv	1253	20/53
	Cell 2 Measurements - Tenth Photovoltaic Load clear - C10 discharge.csv	1258	20/58
	Cell 2 Measurements - Ninth Photovoltaic Load Cloudy - C10 discharge.csv	1253	20/53
	Cell 2 Measurements - Tenth Photovoltaic Load Cloudy - C10 discharge.csv	1258	20/58
	Cell 2 Measurements - Eleventh Load - GC discharge.csv	8162	136/02
	Cell 2 Measurements - Twelfth Photovoltaic Load Clear - GC discharge.csv	2121	35/21
	Cell 2 Measurements - Twelfth Photovoltaic Load Cloudy - GC discharge.csv	2121	35/21
	Cell 2 Measurements - Thirteenth Load wind energy - GC discharge.csv	2816	46/56
	Cell 2 Measurements - Fourteenth Load - Discharge Pulses.csv	5916	98/36
3	Cell 3 Measurements - First Charge-C20 discharge.csv	13,385	223/05
	Cell 3 Measurements - Second Charge-C20 discharge.csv	9905	165/05
	Cell 3 Measurements - Third Charge-C20 discharge.csv	8502	141/42
	Cell 3 Measurements - Fourth Load-C20 discharge.csv	9878	164/38
	Cell 3 Measurements - Fifth Load-C10 discharge.csv	9389	156/29
	Cell 3 Measurements - Sixth Load-C10 discharge.csv	10,153	169/13
	Cell 3 Measurements - Seventh Photovoltaic Load clear - C20 discharge.csv	1849	30/49
	Cell 3 Measurements - Eighth Photovoltaic Load clear - C20 discharge.csv	1895	31/35

(*continued on next page*)

Table 2b (*continued*)

Cell	File	Number of records	Duration (Hour/min.)
	Cell 3 Measurements - Seventh Photovoltaic Load Cloudy - C20 discharge.csv	1849	30/49
	Cell 3 Measurements - Eighth Photovoltaic Load Cloudy - C20 discharge.csv	1895	31/35
	Cell 3 Measurements - Ninth Photovoltaic Load clear - C10 discharge.csv	1253	20/53
	Cell 3 Measurements - Tenth Photovoltaic Load clear - C10 discharge.csv	1258	20/58
	Cell 3 Measurements - Ninth Photovoltaic Load Cloudy - C10 discharge.csv	1253	20/53
	Cell 3 Measurements - Tenth Photovoltaic Load Cloudy - C10 discharge.csv	1258	20/58
	Cell 3 Measurements - Eleventh Load - GC discharge.csv	8162	136/02
	Cell 3 Measurements - Twelfth Photovoltaic Load Clear - GC discharge.csv	2121	35/21
	Cell 3 Measurements - Twelfth Photovoltaic Load Cloudy - GC discharge.csv	2121	35/21
	Cell 3 Measurements - Thirteenth Load wind energy - GC discharge.csv	2816	46/56
	Cell 3 Measurements - Fourteenth Load - Discharge Pulses.csv	5916	98/36
4	Cell 4 Measurements - First Charge-C20 discharge.csv	13,385	223/05
	Cell 4 Measurements - Second Charge-C20 discharge.csv	9905	165/05
	Cell 4 Measurements - Third Charge-C20 discharge.csv	8502	141/42
	Cell 4 Measurements - Fourth Load-C20 discharge.csv	9878	164/38
	Cell 4 Measurements - Fifth Load-C10 discharge.csv	9389	156/29
	Cell 4 Measurements - Sixth Load-C10 discharge.csv	10,153	169/13
	Cell 4 Measurements - Seventh Photovoltaic Load clear - C20 discharge.csv	1849	30/49
	Cell 4 Measurements - Eighth Photovoltaic Load clear - C20 discharge.csv	1895	31/35
	Cell 4 Measurements - Seventh Photovoltaic Load Cloudy - C20 discharge.csv	1849	30/49
	Cell 4 Measurements - Eighth Photovoltaic Load Cloudy - C20 discharge.csv	1895	31/35
	Cell 4 Measurements - Ninth Photovoltaic Load clear - C10 discharge.csv	1253	20/53
	Cell 4 Measurements - Tenth Photovoltaic Load clear - C10 discharge.csv	1258	20/58
	Cell 4 Measurements - Ninth Photovoltaic Load Cloudy - C10 discharge.csv	1253	20/53
	Cell 4 Measurements - Tenth Photovoltaic Load Cloudy - C10 discharge.csv	1258	20/58
	Cell 4 Measurements - Eleventh Load - GC discharge.csv	8162	136/02
	Cell 4 Measurements - Twelfth Photovoltaic Load Clear - GC discharge.csv	2121	35/21
	Cell 4 Measurements - Twelfth Photovoltaic Load Clear - GC discharge.csv	2121	35/21
	Cell 4 Measurements - Thirteenth Load wind energy - GC discharge.csv	2816	46/56
	Cell 4 Measurements - Fourteenth Load - Discharge Pulses.csv	5916	98/36
5	Cell 5 Measurements - First Charge-C20 discharge.csv	13,385	223/05
	Cell 5 Measurements - Second Charge-C20 discharge.csv	9905	165/05
	Cell 5 Measurements - Third Charge-C20 discharge.csv	8502	141/42
	Cell 5 Measurements - Fourth Load-C20 discharge.csv	9878	164/38
	Cell 5 Measurements - Fifth Load-C10 discharge.csv	9389	156/29
	Cell 5 Measurements - Sixth Load-C10 discharge.csv	10,153	169/13
	Cell 5Measurements - Seventh Photovoltaic Load clear - C20 discharge.csv	1849	30/49
	Cell 5 Measurements - Eighth Photovoltaic Load clear - C20 discharge.csv	1895	31/35
	Cell 5 Measurements - Seventh Photovoltaic Load Cloudy - C20 discharge.csv	1849	30/49
	Cell 5 Measurements - Eighth Photovoltaic Load Cloudy - C20 discharge.csv	1895	31/35
	Cell 5 Measurements - Ninth Photovoltaic Load clear - C10 discharge.csv	1253	20/53
	Cell 5 Measurements - Tenth Photovoltaic Load clear - C10 discharge.csv	1258	20/58
	Cell 5 Measurements - Ninth Photovoltaic Load Cloudy - C10 discharge.csv	1253	20/53
	Cell 5 Measurements - Tenth Photovoltaic Load Cloudy - C10 discharge.csv	1258	20/58
	Cell 5 Measurements - Eleventh Load - GC discharge.csv	8162	136/02
	Cell 5 Measurements - Twelfth Photovoltaic Load Clear - GC discharge.csv	2121	35/21
	Cell 5 Measurements - Twelfth Photovoltaic Load Cloudy - GC discharge.csv	2121	35/21
	Cell 5 Measurements - Thirteenth Load wind energy - GC discharge.csv	2816	46/56
	Cell 5 Measurements - Fourteenth Load - Discharge Pulses.csv	5916	98/36
6	Cell 6 Measurements - First Charge-C20 discharge.csv	13,385	223/05
	Cell 6 Measurements - Second Charge-C20 discharge.csv	9905	165/05
	Cell 6 Measurements - Third Charge-C20 discharge.csv	8502	141/42
	Cell 6 Measurements - Fourth Load-C20 discharge.csv	9878	164/38
	Cell 6 Measurements - Fifth Load-C10 discharge.csv	9389	156/29
	Cell 6 Measurements - Sixth Load-C10 discharge.csv	10,153	169/13
	Cell 6 Measurements - Seventh Photovoltaic Load clear - C20 discharge.csv	1895	31/35
	Cell 6 Measurements - Eighth Photovoltaic Load clear - C20 discharge.csv	1895	31/35

(*continued on next page*)

Table 2b (*continued*)

Cell	File	Number of records	Duration (Hour/min.)
	Cell 6 Measurements - Seventh Photovoltaic Load Cloudy - C20 discharge.csv	1849	30/49
	Cell 6 Measurements - Eighth Photovoltaic Load Cloudy - C20 discharge.csv	1895	31/35
	Cell 6 Measurements - Ninth Photovoltaic Load clear - C10 discharge.csv	1253	20/53
	Cell 6 Measurements - Tenth Photovoltaic Load clear - C10 discharge.csv	1258	20/58
	Cell 6 Measurements - Ninth Photovoltaic Load Cloudy - C10 discharge.csv	1253	20/53
	Cell 6 Measurements - Tenth Photovoltaic Load Cloudy - C10 discharge.csv	1258	20/58
	Cell 6 Measurements - Eleventh Load - GC discharge.csv	8162	136/02
	Cell 6 Measurements - Twelfth Photovoltaic Load Clear - GC discharge.csv	2121	35/21
	Cell 6 Measurements - Twelfth Photovoltaic Load Cloudy - GC discharge.csv	2121	35/21
	Cell 6 Measurements - Thirteenth Load wind energy - GC discharge.csv	2816	46/56
	Cell 6 Measurements - Fourteenth Load - Discharge Pulses.csv	5916	98/36

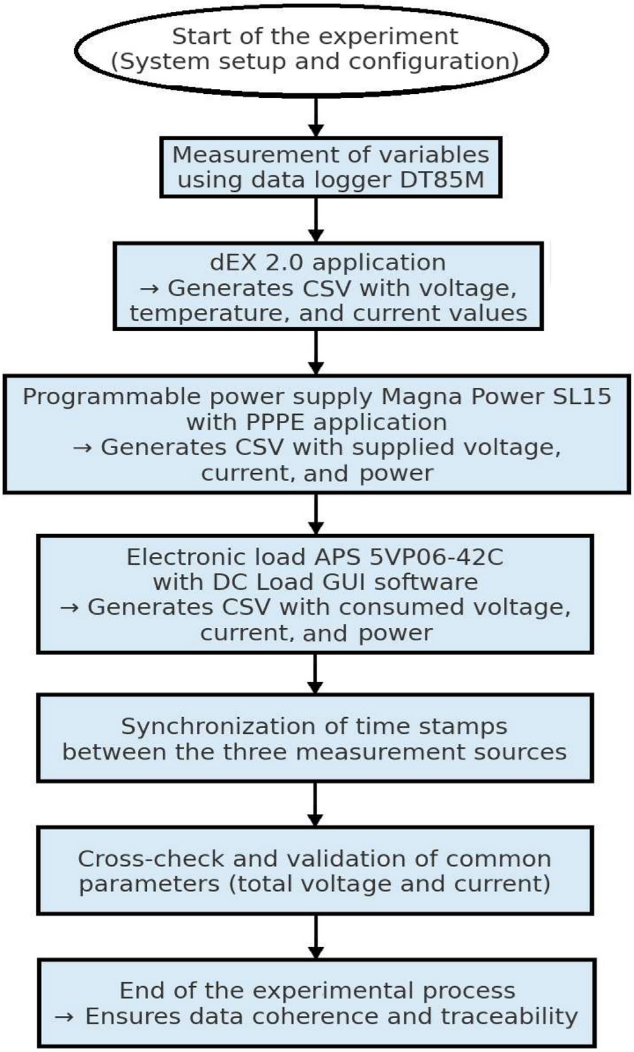

Fig. 8. Flowchart of the experimental procedure and data acquisition process.

In summary, the experimental setup combined high-capacity OPzS batteries, programmable charging and discharging systems, calibrated monitoring equipment, and robust data acquisition tools. This configuration enabled controlled yet realistic operating conditions, ensuring a comprehensive dataset suitable for modeling, validation, and energy management studies.

All values from these sources were synchronized to ensure full coherence and traceability across the experimental records. Fig. 8 has been included to illustrate the overall data acquisition and synchronization process.

Limitations

The main limitation during data acquisition was related to laboratory safety protocols . These refer to inactivity periods between charge and discharge phases, which occurred because, for safety reasons, tests could only be performed under the supervision of technical staff.

These inactive periods are reflected in the current measurements, where the recorded current value is 0 A. In continuous operation cycles, by contrast, the current transitions smoothly from positive values (charging) to negative values (discharging). No artificial correction or filtering has been applied to these data, as they represent actual operating conditions during the experimental procedure. The overall dataset remains comprehensive, reliable, and suitable for modeling, validation, and comparative studies.

Ethics Statement

The authors confirm that they have read and followed the ethical requirements for publication in Data in Brief. This work does not involve human subjects, animal experiments, or data collected from social media platforms.

CRediT Author Statement

Javier Rocha: Conceptualization, Methodology, Validation, Investigation, Resources, Data Curation, Writing - Original Draft, Visualization. **Ricardo Aguasca-Colomo:** Conceptualization, Methodology, Validation, Investigation, Resources, Writing - Review & Editing, Supervision, Project administration, Funding acquisition. **Máximo Méndez:** Conceptualization, Methodology, Software, Validation, Formal analysis, Investigation, Writing - Review & Editing, Supervision, Project administration.

Data Availability

Experimental Dataset Patterns in a 1200Ah Battery (Original data) (Zenodo).

Acknowledgments

The authors would like to thank the Government of the Canary Islands for funding the acquisition of most of the equipment used in this project: EIS 2021-04 – CPG:6405053 – SI:1825. This funding was provided as part of Action 2: Instrumentation for optimizing the management of renewable energy systems, within the project Scientific computing infrastructure for applications of artificial intelligence and numerical simulation in the environment and management of renewable energy (IUSIANI-ODS). The project was supported through a direct subsidy granted to the University of Las Palmas de Gran Canaria by Order No 459 of the Ministry of Economy, Knowledge and Employment of the Government of the Canary Islands, processed by the Canary Islands Agency for Research, Innovation and Information Society. The subsidy was co-financed by the European Regional Development Fund (ERDF) at a rate of 85 % under the Canary Islands ERDF Operational Programme 2014–2020. The authors also gratefully acknowledge the contribution of the technical staff who assisted in the experimental setup and monitoring process.

Declaration of Competing Interest

The authors declare that they have no known competing financial interests or personal relationships that could have appeared to influence the work reported in this paper.

References

[1] J.B. Copetti, P. García-Velasco, J.A. Olasolo, L. Prieto, A general battery model PV system simulation, Prog. Photovolt.: Res. Appl. 1 (4) (1993) 283–292, doi:10.1002/pip.4670010405.
[2] S. Blaifi, S. Moulahoum, I. Colak, W. Merrouche, An enhanced dynamic model of battery using genetic algorithm suitable for photovoltaic applications, Appl. Energy. 169 (2016) 888–898, doi:10.1016/j.apenergy.2016.02.062.
[3] D. Guasch, J. Silvestre, Dynamic battery modelling for photovoltaic applications, Prog. Photovolt: Res. Appl. 11 (3) (2003) 193–206, doi:10.1002/pip.480.
[4] F.J. Rocha, J.M. Cabrera, R. Aguasca, M. Mendez, P. Rivera-Rodríguez, Analysis of a lead-acid battery storage system connected to the DC bus of a four quadrants converter to a microgrid, Renew. Energy Power Qual. J. 17 (1) (2019) 151–154, doi:10.24084/repqj17.249.
[5] A.B. Khan, A.S. Akram, W. Choi, State of charge estimation of flooded lead acid battery using adaptive unscented kalman filter, Energies 17 (6) (2024) 1275 Art, doi:10.3390/en17061275.
[6] H. Rezk, S. Ferahtia, R.M. Ghoniem, A. Fathy, M.M. Ghoniem, R. Alkanhel, Robust parameter identification strategy for lead-acid battery model, Batteries 8 (12) (2022) 283 Art, doi:10.3390/batteries8120283.
[7] J. Olarte, J. Martinez de Ilarduya1, E. Zulueta, R. Ferret1, J. Garcia-Ortega, J.M. Lopez-Guede, Online identification of VLRA battery model parameters using electrochemical impedance spectroscopy, Batteries 8 (2022) 238 Art, doi:10.3390/batteries8110238.
[8] J. Loukil, F. Masmoudi, N. Derbel, A real-time estimator for model parameters and state of charge of lead acid batteries in photovoltaic applications, J. Energy Stor. 34 (2021) 102184, doi:10.1016/j.est.2020.102184.
[9] Y. Fan, Q. Lin, R. Huang, Non-invasive method-based estimation of battery State-of-health with dynamical response characteristics of load surges, Energies 17 (3) (2024) 583 Art, doi:10.3390/en17030583.
[10] M. Becherif, H.-S. Ramadan, A. Benmouna, S. Jemei, Initial State of charge estimation of battery using impedance measurement and hybrid methods, Int. J. Energy Res. /Relat. Publ. 53 (2022) 102727 Part C, doi:10.1016/j.seta.2022.102727.
[11] S. Jiang, Z. Song, A review on the state of health estimation methods of lead-acid batteries, J. Power Sourc. 517 (2022) 230710, doi:10.1016/j.jpowsour.2021.230710.
[12] D. Selvabharathi, N. Muruganantham, Estimating the State of health of lead-acid battery using cycle-counting and machine-learning approaches, Int. J. Energy Power. Eng. /World. Sci. (2022), doi:10.1142/S0218126622500815.